Chalcogenide Letters Vol. 18, No. 10, October 2021, p. 617 - 628

Color tunable Gd_2O_3: Tb^{3+}/Eu^{3+} nano-phosphors prepared via laser ablation in water

H. W Deng, D. H. Chen*
State Key Laboratory of Optoelectronic Materials and Technologies, School of Electronics and Information Technology, Sun Yat-sen University, Guangzhou 510275, P. R. China

Gd_2O_3 has been considered as a kind of good host material for photoluminescence. The method of laser ablation in liquid (LAL) is increasingly used for the preparation of Gd_2O_3 because it is green and usually simple. In this work, monoclinic Gd_2O_3:Tb^{3+}/Eu^{3+} nano-phosphors were successfully synthesized by LAL method. The morphology, structure, and optical properties of the nano-phosphors were discussed. The color of fluorescence of Gd_2O_3:Tb^{3+}/Eu^{3+} nano-phosphors were successfully turned by controlling the content of Tb^{3+} and Eu^{3+}. The results show that the synthesized Gd_2O_3:Tb^{3+}/Eu^{3+} nano-phosphors are potential to be applied to display, lighting, biological imaging or other fields.

(Received May 19, 2021; Accepted October 14, 2021)

Keywords: Gadolinium oxide, Photoluminescence, Nano-phosphors, Laser ablation in liquid

1. Introduction

Lanthanide-doped phosphors have attracted much attention from researchers in recent years due to the unique electronic structure of lanthanides. [1] To date, lanthanide-doped phosphors have been widely applied to lighting [2], display [3], biological imaging [4], temperature sensing [5], information storage, [6] fingerprinting, [7] anti-counterfeiting, [8] and other fields because of the characteristics of excellent photostability, narrow emission peaks, long lifetimes, large Stokes shifts and minimized photobleaching. It is well known that Tb^{3+} ion is regarded as a promising green-emitting activator and Eu^{3+} ion is regarded as a promising red-emitting activator. [9-11] However, it is difficult for single doped phosphors to achieve rich multicolor luminescence. Therefore, Tb^{3+} ions and Eu^{3+} ions co-doped phosphor is a good choice for color tunable luminescence by simply adjusting the ratio of Tb^{3+} ions and Eu^{3+} ions. [12-15] Besides, the choice of the host matrix of the lanthanide-doped phosphor is also very important. Gadolinium oxide has been considered as a kind of good host material for photoluminescence. [15-18] On the one hand, the trivalent Gd ions can be easily replaced by other lanthanide ions to achieve substitutional doping. [18] On the other hand, gadolinium oxide has lower phonon energy and good chemical stability. [19] In addition, the preparation condition of gadolinium oxide is usually simple，gadolinium oxide can be prepared in air or water environment. [20] The traditional

* Corresponding author: stscdh@mail.sysu.edu.cn
https://doi.org/10.15251/CL.2021.1810.617

methods of preparing gadolinium oxide mainly are hydrothermal method [21], homogeneous precipitation method [22], sol-gel method [23], combustion method [24] and solid-state method [25]. Those methods require either high-purity chemical reagents or strict reaction conditions, and some of them inevitably generate by-products. In recent years, laser ablation in liquid (LAL) has been a promising method for synthesizing oxide nanoparticles (NPs). [26-31] Oxide NPs can be synthesized at room temperature and normal pressure by this approach. Besides, laser-generated NPs are usually highly pure and ligands-free because usually no chemical precursors, chelating agents or coordinating molecules are required in the preparation process. [26] It is worth mentioning that the LAL method can easily prepare monoclinic gadolinium oxide nanoparticles. [32] To date, the most popular methods for preparing monoclinic gadolinium oxide are solid-state method and combustion method. [16] Compared with combustion method, the nanoparticles prepared by LAL method are easier to collect because nanoparticles are prepared in liquid environment. Furthermore, the solid-state method usually requires a long time of grinding to obtain nano or micro materials. In this work, color tunable monoclinic Gd_2O_3:Tb^{3+}/Eu^{3+} nano-phosphors were synthesized by LAL method. The microstructure, morphology, composition and properties of fluorescence of these nano-phosphors were fully studied. The results show that synthesized nano-phosphors are potential to be applied to display, lighting biological imaging or other field due to the property of tunable light.

2. Experimental details

2.1. Material synthesis

Nanomaterials were prepared in two steps. The first step is to prepare ceramic targets using conventional solid-state method. The ceramic targets were synthesized according to stoichiometric compositions of $(1-x-y)Gd_2O_3$-xEu_2O_3-yTb_2O_3 in mole ratio. In the actual experiment, $(x/2)Tb_4O_7$ was used instead of xTb_2O_3. The raw materials used to prepare ceramic targets are Gd_2O_3 (99.99%), Eu_2O_3 (99.99%) and Tb_4O_7 (99.99%) purchased from Aladdin. First, the raw materials were thoroughly mixed by grinding according to the designed molar ratio, and then they were mixed with an appropriate amount of PVA (10 wt %) solution. Until the sticky powders were dry, they were uniaxially pressed into disks , and then the disks were sintered at 1550 °C for 6 hours. After natural cooling, the ceramic targets were finally obtained. The second step is laser ablating the prepared target. The experimental setup of LAL is schematically shown in Fig. 1. The ceramic target was placed on the bottom of a beaker and covered by 5 mm deionized water. Then, a beam of laser was focused on the target (wavelength = 532 nm, pulse duration = 5 ns, focal length = 200 mm, pulse power = 90 mJ, repetition rate = 5 Hz). After ablation, the obtained colloid solution was collected for further experiment.

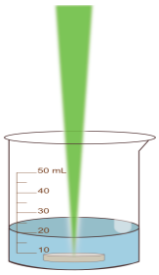

Fig. 1. Schematic diagram of pulsed laser ablation in liquid.

2.2 Characterization

The morphology of the prepared nano-phosphors was observed with a FEI Tecnai G2 F30 transmission electron microscope (TEM) operating at an accelerating voltage of 300 kV. The phase structures of samples were characterized by an x-ray diffraction diffractometer (XRD, Rigaku, SmartLabx) with Cu kα radiation (λ=1.54 Å, 46 kV, 30mA). Fluorescence characteristics were measured by a photoluminescence spectrometer (FLS980, Edinburgh). In the measurement of excitation spectrum and emission spectrum, a 300 W xenon lamp was used as the excitation light source. The fluorescence decay was measured by time-correlated single photon counting method, and a millisecond flashlamp (uF900, 100 Hz) was used as the excitation light source.

3. Results and discussion

The XRD patterns of three representative samples (Gd_2O_3:5%Eu, Gd_2O_3:5%Tb and Gd_2O_3:5%Tb,5%Eu) prepared by LAL method are shown in Fig.2. The peak positions of those samples match the standard monoclinic gadolinium oxide (PDF-42-1465). Meanwhile, no obvious signal of other phase could be detected at the limit of detection by XRD. It shows that the crystal structure of Gd_2O_3 has not changed. It can be attributed to the fact that the radii of Gd^{3+} ion (0.938 Å), Tb^{3+} ion (0.923 Å) and Eu^{3+} ion (0.947 Å) are very close. A transmission electron microscope (TEM) image of Gd_2O_3:5%Eu,5%Tb powders prepared by LAL method is shown in Fig.3. It can be seen from the image that the prepared powders are nanoscale.

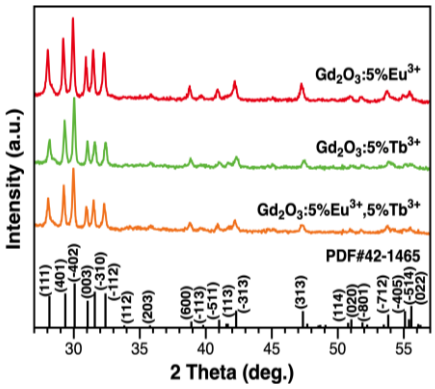

Fig. 2. XRD patterns of the as-prepared Gd_2O_3:5%Tb^{3+}, Gd_2O_3:5%Eu^{3+} and Gd_2O_3: 5%Tb^{3+},5% Eu^{3+}, and the corresponding standard data of monoclinic Gd_2O_3 (PDF No. 42-1465).

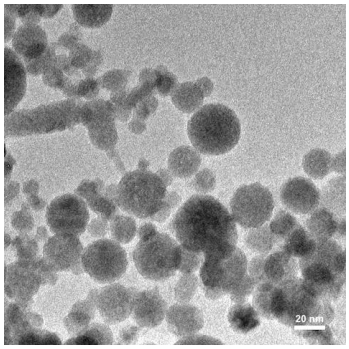

Fig. 3. Typical TEM image of Gd_2O_3: 5%Tb^{3+},5%Eu^{3+} nano-phosphors.

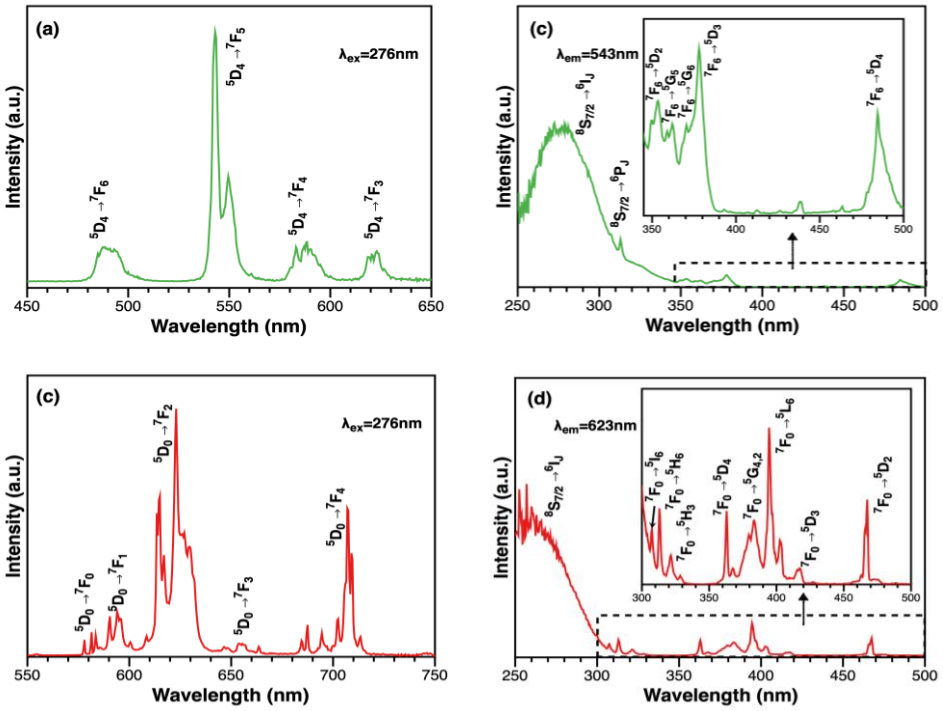

Fig. 4. (a) and (c) emission spectra of Gd_2O_3: 5% Tb nano-phosphors and Gd_2O_3: 5% Eu nano-phosphors ($\lambda_{ex} = 276\ nm$), (b) and (d) excitation spectra of Gd_2O_3: 5% Tb nano-phosphors and Gd_2O_3: 5% Eu nano-phosphors ($\lambda_{em} = 543\ nm$ and $\lambda_{em} = 623\ nm$, respectively).

The emission spectrum of Gd_2O_3:5%Eu nano-phosphors under the excitation of 276 nm and the excitation spectrum monitored at 623 nm are shown in Fig.4 (a). There are mainly 5 characteristic emission peaks in the emission spectrum. The emission peaks at 583 nm, 591 nm, 623 nm, 654 nm and 707 nm respectively correspond to $^5D_0 \rightarrow {}^7F_J$ (J=0, 1, 2, 3, 4) transitions of Eu^{3+} ion. In the excitation spectrum, the absorption peak at 276 nm corresponds to the ($^8S_{7/2} \rightarrow {}^6I_{9/2}$) electronic transition of Gd^{3+} ion, and absorption peaks at 308 nm, 313 nm, 322 nm, 363 nm, 379 nm, 383 nm, 394 nm, 417 nm and 467 nm correspond to $^6F_0 \rightarrow {}^5I_6$, $^7F_0 \rightarrow {}^5H_6$, $^7F_0 \rightarrow {}^5H_3$, $^7F_0 \rightarrow {}^5D_4$, $^7F_0 \rightarrow {}^5G_4$, $^7F_0 \rightarrow {}^5G_2$, $^7F_0 \rightarrow {}^5L_6$, $^7F_0 \rightarrow {}^5D_2$ and $^7F_0 \rightarrow {}^5D_2$ transitions of Eu^{3+} ion. The emission spectrum of Gd_2O_3:5%Tb nano-phosphors under the excitation of 276 nm and the excitation spectrum monitored at 543 nm are shown in Fig.4 (b). There are mainly 4 characteristic

emission peaks in the emission spectrum. Those peaks are basically consistent with the characteristic peaks of Tb^{3+} ion reported in the previous literatures. [33, 34] This confirms the presence of Tb^{3+} ion. The emission peaks at 488 nm, 543 nm, 588 nm and 623 nm respectively correspond to $^5D_4 \rightarrow {}^7F_J$ (J=6,5,4,3) transitions of Tb^{3+} ion. In the excitation spectrum, the absorption peaks at 276 nm and 313 nm correspond to $^8S_{7/2} \rightarrow {}^6I_{9/2}$ and $^8S_{7/2} \rightarrow {}^6P_J$ electronic transition of Gd^{3+} ion, and absorption peaks at 353 nm, 362 nm, 370 nm, 378 nm and 485 nm correspond to $^7F_6 \rightarrow {}^5D_2$, $^7F_6 \rightarrow {}^5G_5$, $^7F_6 \rightarrow {}^5G_6$, $^7F_6 \rightarrow {}^5D_3$ and $^7F_6 \rightarrow {}^5D_4$ transitions of Tb^{3+} ion. Figure 5 shows the emission spectra of Gd_2O_3:xTb (x=0.1%, 3%, 5%, 7%, 15%, 25%) nano-phosphors under excitation of 276 nm, and the inset shows the trend of intensity of the strongest peak at 543 nm. The fluorescence intensity first increases and then decreases. This phenomenon can be explained as follows. The probability of energy transfer from Gd^{3+} ions to Tb^{3+} ions would increase with the increase of Tb concentration in condition of lower doping concentration, therefore the number of excited Tb^{3+} ions would increase, which results in the increase of fluorescence intensity. As the concentration of Tb continuously increases, the probability of energy transfer between Tb ions would increase, which will increase the probability of energy transfer to the fluorescence quenching area, resulting in decrease of fluorescent intensity. Among all Gd_2O_3: xTb nano-phosphors we prepared, the fluorescence of Gd_2O_3: 5%Tb is the strongest. Therefore, we choose the ratio of 5%Tb for co-doping with different ratio of Eu for turning fluorescent color. We prepared Gd_2O_3:5%Tb,yEu (y= 0.1%, 1%, 3% and 5%) nano-phosphors by LAL method. The emission spectra of Gd_2O_3:5%Tb:yEu nano-phosphors under excitation of 276 nm are shown in Fig,6. It can be seen from Fig.6 that with the increase of Eu ratio, the intensity of characteristic emission peak of Tb^{3+} ion decreases, and the intensity of characteristic emission peak of Eu^{3+} ion increases. In our opinion, the decrease of peak intensity of Tb^{3+} ion can be attributed to the existence of energy transfer from Tb^{3+} ions to Eu^{3+} ions.

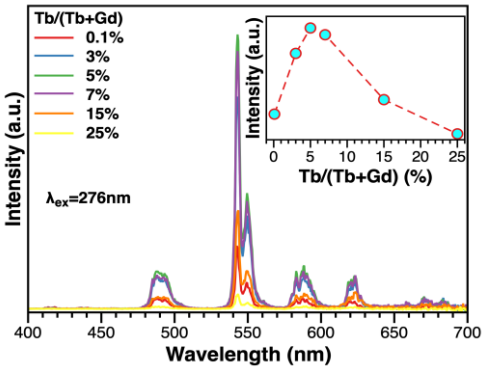

Fig. 5. Emission spectra of Gd_2O_3:xTb (x=0.1%, 3%, 5%, 7%, 15%, 25%) nano-phosphors under 276nm excitation.

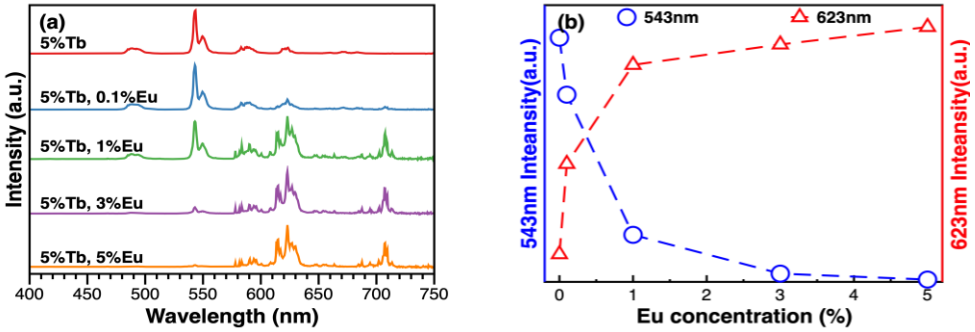

Fig. 6. (a) Emission spectra of Gd_2O_3:5%Tb,xEu nano-phosphors. (b) Emission intensity of Eu^{3+} ions at 623nm as a function of Eu content.

In order to verify whether there is a phenomenon of energy transfer from Tb^{3+} ions to Eu^{3+} ions, we compared the excitation spectra of Gd_2O_3:5%Tb,5%Eu , Gd_2O_3:5%Eu and Gd_2O_3:5%Tb monitored at 707 nm, and the excitation spectra are shown in Fig.7. It can be found that when monitored at 707 nm, the excitation spectra of Gd_2O_3:5%Eu nano-phosphors and Gd_2O_3:5%Tb nano-phosphors have no absorption peak at 353 nm and 485 nm, but in excitation spectrum of Gd_2O_3: 5%Tb,5%Eu there are absorption peaks at 353 nm and 485 nm. As it is shown in Fig.4 the peaks at 353 nm and 485 nm are characteristic absorption peaks of Tb^{3+} ion, and the peak at 707 nm is a characteristic emission peak of Eu^{3+} ion. In other words, the Gd_2O_3:5%Tb,5%Eu nano-phosphors can emit characteristic light of Eu^{3+} ion under the excitation of characteristic excitation wavelength of Tb^{3+} ion. This is an evidence of energy transfer from Tb^{3+} ions to Eu^{3+} ions.

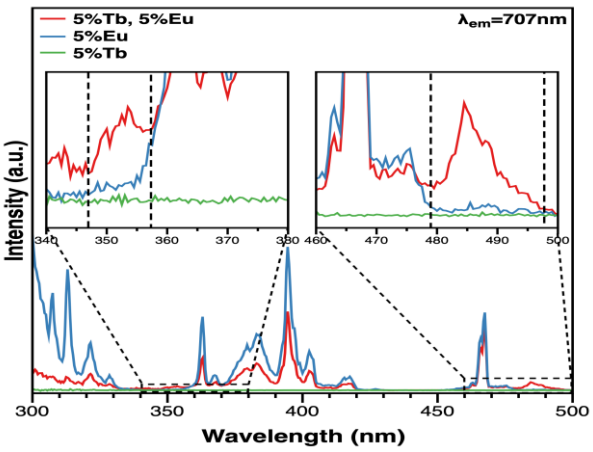

Fig. 7. Excitation spectra of Gd_2O_3:5%Tb nano-phosphors, Gd_2O_3:5%Eu nano-phosphors and Gd_2O_3:5%Tb, 5%Eu nano-phosphors. ($\lambda_{em} = 707\ nm$).

In order to further investigate the energy transfer process, the fluorescence lifetime of 543 nm (strongest characteristic emission wavelength of Tb^{3+} ion) of Gd_2O_3:5%Tb,yEu (y= 0, 0.1%, 1%, 3% and 5%) nano-phosphors under the excitation of 276 nm had been measured. The results

are shown in Fig.8. The decay curve of sample Gd_2O_3:5%Tb nano-phosphors conforms to single exponential fitting [35]:

$$I = I_0 + Ae^{-t/\tau}, \#(1)$$

where I is fluorescent intensity which is proportional to the counts in Fig.8, t is decay time, τ is fitted lifetime, I_0 and A are constant.

The decay curves of sample Gd_2O_3:5%Tb, yEu (y= 0.1%, 1%, 3% and 5%) nano-phosphors conform to double exponential fitting[36]:

$$I = I_0 + A_1e^{-t/\tau_1} + A_2e^{-t/\tau_2}, \#(2)$$

where I is fluorescent intensity which is proportional to the counts in Fig.8, t is decay time, τ_1 and τ_2 are fitted lifetime, I_0, A_1 and A_2 are constant.

The average lifetime values are calculated by the following formula [36]:

$$\tau_{av} = \frac{A_1\tau_1^2 + A_2\tau_2^2}{A_1\tau_1 + A_2\tau_2}. \#(3)$$

In our opinion, the fluorescence decay includes two types. One is the radiative relaxation of Tb^{3+} ions, and the other corresponds to the energy transfer from Tb^{3+} ions to Eu^{3+} ions. Additionally, the average lifetime of characteristic emission peak of Tb^{3+} decreases with the increase of the amount of Eu increases. The results of fluorescence lifetime show the existence of energy transfer process from Tb^{3+} to Eu^{3+} ions.

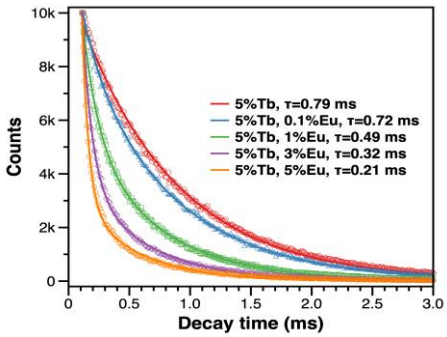

Fig. 8. Decay curves and lifetime values of Gd_2O_3:5%Tb, xEu (x=0, 0.1%, 1%, 3%, 5%) nano-phosphors. $(\lambda_{ex} = 276nm, \lambda_{em} = 623nm)$.

The energy transfer efficiency can be roughly calculated from the intensity of the emitted light:[36]

$$\eta_T = 1 - \frac{I}{I_0}, \#(4)$$

where I and I_0 correspond to the luminescence intensity of Tb^{3+} ions with and without Eu^{3+} ions, respectively. As it is shown in Fig.9, the energy transfer efficiency increases gradually with the increase of Eu ratio.

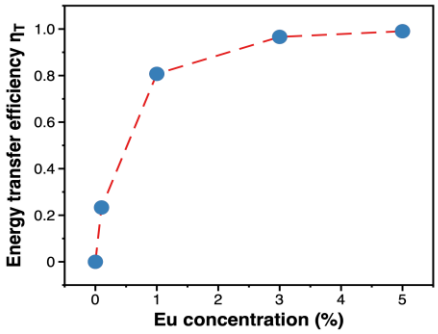

Fig. 9. Energy transfer efficiency (η_T) as a function of Eu concentration.

The energy transfer mechanism between rare earth ions is related to the distance between rare earth ions. The average distance R of Tb^{3+} and Eu^{3+} ions can be calculated by using the concentration quenching method [37]:

$$R = 2 \times \left[\frac{3V}{4\pi\chi_{Tb+Eu}Z}\right]^{1/3}, \#(5)$$

where V is the volume of the unit cell, χ_{Tb+Eu} is the total doping concentration of Tb^{3+} ions and Eu^{3+} ions, and Z is the number of available crystallographic sites occupied by the activator ions in the unit cell. For the monoclinic Gd_2O_3 host lattice, $V = 435.2\ Å^3$ and $Z = 6$. The average distance R is determined to be 13.95 Å, 13.22 Å, 12.01 Å and 11.15 Å for $\chi_{Tb+Eu} = 0.051, 0.06, 0.08, \text{and } 0.10$, respectively. Critical concentration is defined as the concentration of Tb and Eu when the characteristic fluorescence intensity of Tb is equal to half of characteristic fluorescence intensity of Gd_2O_3:5%Tb. Substituting the critical concentration into the χ_{Tb+Eu} in formula (4), the result is critical distance. It is obvious that the sum of the concentrations is between 0.051 and 0.10, that is, the critical distance is between 11.15 Å and 13.95 Å. It is well known that there are two possible interactions for resonant energy transfer: exchange interaction and multipolar interaction. The exchange interaction requires that the critical distance between the donor and the acceptor should be shorter than 5 Å. In our case, the critical distance is between 11.15 and 13.95. Therefore, the interaction mode of energy transfer is more likely to be multipolar interaction. According to Dexter's energy transfer formula of multipolar interaction and Reisfeld's approximation, the following equation can be used to analyze the potential mechanism [38]:

$$\frac{I_{SO}}{I_S} \propto C_{Tb+Eu}^{n/3}, \#(6)$$

where I_{SO} is the intrinsic luminescence intensity of Tb^{3+} ion; I_S is the luminescence intensity of Tb^{3+} ion in the presence of Eu^{3+} ion; C_{Tb+Eu} is the sum of the concentration of Tb^{3+} ion and Eu^{3+} ion. The value of n (6, 8, or 10) correspond to the dipole–dipole interaction, dipole–quadrupole interaction, or quadrupole–quadrupole interaction, respectively. The dependence of I_{SO}/I_S of Tb^{3+} on $C_{Tb+Eu}^{n/3}$ and the corresponding linear fitting results are shown in Fig. 10. When n = 10,

the plots can be better linearly fitted, which implies that the interaction of Eu^{3+} ions and Tb^{3+} ions is predominated by quadrupole–quadrupole interaction.

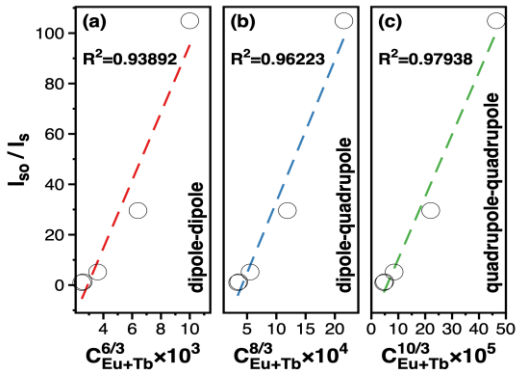

Fig. 10. Dependence of I_{so}/I_s on $C_{Eu+Tb}^{(n/3)}$ (n=6,8,10) of Gd_2O_3:5%Tb,xEu (x=0.1%, 1%, 3%, 5%) nano-phosphors.

The possible schematic diagram of energy transfer for Gd_2O_3 :Tb^{3+},Eu^{3+} nano-phosphors is shown in Fig.11. Under the excitation of 276 nm, ground-state ($^8S_{7/2}$) electrons of Gd^{3+} ions absorb photons and populate the excited states (^6I_J). The electrons in the excited state ^6I_J can easily relax to the lower excited state ^6P_J via no-radiative relaxation process. Then, the energy can transfer from Gd^{3+} ions to Tb^{3+} ions and Eu^{3+} ions because the excited state ^6P_J of Gd^{3+} ion is slightly higher energy than the excited state $^5D_4$ of Eu^{3+} ion and the excited state $^5D_2$ of Tb^{3+} ions. The excited electrons in $^5D_4$ of Eu^{3+} and $^5D_2$ of Tb^{3+} ions can easily relax to the lower state $^5D_0$ of Eu^{3+} and $^5D_4$ of Tb^{3+}, respectively, via non-radiative process because the higher excited states are unstable. The energy can transfer from Tb^{3+} ions to Eu^{3+} ions because the excited state $^5D_4$ of Tb^{3+} ion is slightly higher energy than the excited state $^5D_0$ of Eu^{3+} ion, this is the reason why the characteristic fluorescence intensity of Tb^{3+} ion decreases when Eu and Tb are co-doped. Finally, the electrons in the excited state $^5D_0$ of Eu^{3+} and $^5D_4$ of Tb^{3+} return to the relevant ground states through photon emission.

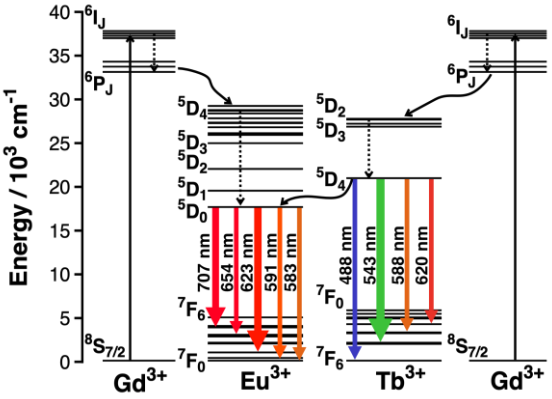

Fig. 11. The possible scheme of energy transfer process of Gd_2O_3:Eu^{3+},Tb^{3+} nano-phosphors.

Figure 12 is the CIE chromaticity diagram of Gd_2O_3:5%Tb,xEu (x=0, 0.1%, 1%, 3%, 5%) nano-phosphors under the excitation of 276 nm. The corresponding CIE chromaticity coordinates calculated from emission spectra are (0.36, 0.57), (0.39, 0.55), (0.52, 0.44), (0.62, 0.36) and (0.65, 0.34). It can be seen from Fig.12 that as the Eu concentration increases, the color gradually changes from green to red. The results show that the fluorescent color can be turned by controlling the Eu and Tb ratio of Gd_2O_3 :5%Tb,xEu nano-phosphors.

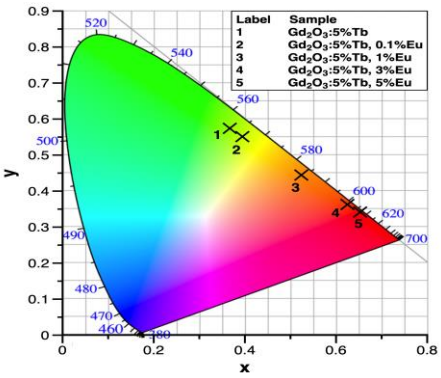

Fig. 12. CIE chromaticity coordinates for Gd_2O_3: 5%Tb, xEu (x=0, 0.1%, 1%, 3%, 5%) nano-phosphors under 276 nm excitation.

4. Conclusion

In summary, we successfully synthesized monoclinic Tb^{3+} and Eu^{3+} doped Gd_2O_3 nano-phosphors by LAL technique. The effect of the concentration of Tb^{3+} ion and Eu^{3+} ion on the fluorescence properties has been studied in detail. The fluorescent color of Gd_2O_3:Tb^{3+},Eu^{3+} nano-phosphors can be turned from green to red by controlling the amount of Tb and Eu. Additionally, the energy transfer mechanism has been fully studied. The results indicate that the Gd_2O_3:Tb^{3+},Eu^{3+} nano-phosphors synthesized by LAL technique are promising candidates for display, lighting, biological imaging or other application.

Acknowledgements

This work was supported by the National Basic Research Program of China (2014CB931700), the National Natural Science Foundation of China under Grant Nos. 81471787 and 61471401.

References

[1] G. Wang, Q. Peng, Y. Li, Accounts of Chemical Research **44**(5), 322 (2011).
[2] B. Liu, J. Li, G. Duan, Q. Li, Z. Liu, Journal of Luminescence **206**, 348 (2019).
[3] E. Downing, L. Hesselink, J. Ralston, R. Macfarlane, Science **273**(5279), 1185 (1996).

[4] Nexha, J. J. Carvajal, M. C. Pujol, F. Diaz, M. Aguilo, Nanoscale **13**(17), 7913 (2021).
[5] F. Vanden Bussche, A. M. Kaczmarek, V. Van Speybroeck, P. Van Der Voort, C. V. Stevens, Chemistry-a European Journal **27**(25), 7214 (2021).
[6] Q. Zhang, S. Yue, H. Sun, X. Wang, X. Hao, S. An, Journal of Materials Chemistry C **5**(15), 3838 (2017).
[7] E. Anderson, M. Johansen, B. O. Erokwu, H. Hu, Y. Gu, Y. Zhang, M. Kavran, J. Vincent, M. L. Drumm, M. A. Griswold, N. F. Steinmetz, M. Li, H. Clark, R. J. Darrah, X. Yu, S. M. Brady-Kalnay and C. A. Flask, Scientific Reports **9**(1), 19888 (2019).
[8] W. Ren, G. Lin, C. Clarke, J. Zhou, D. Jin, Advanced Materials **32**(18), e1901430 (2020).
[9] N. M. Maalej, A. Qurashi, I. Bennour, L. R. Haddada, M. N. Shaikh, M. Ilyas, N. Essoukri Ben Amara, R. Maalej, M. A. Gondal, Methods and Applications in Fluorescence **9**(2), 025002 (2021).
[10] R. Fu, M. G. Ou, C. L. Yang, Y. Y. Hu, H. Yin, Journal of Luminescence **222,** 123180 (2020).
[11] N. Vashistha, A. Chandra, M. Singh, New Journal of Chemistry **44**(33), 14211 (2020).
[12] R. Naik, S. C. Prashantha, H. Nagabhushana, Optical Materials **72**, 295(2017).
[13] S. Nan, F. Hong, H. Xu, J. Dou, G. Liu, X. Dong, J. Wang, W. Yu, Journal of Materials Science: Materials in Electronics **31**(16), 13688 (2020).
[14] H. L. Li, G. X. Liu, J. X. Wang, X. T. Dong, W. S. Yu, Journal of Luminescence **186**, 6 (2017)
[15] Zhu, J. Li, X. Guo, Q. Li, H. Wu, L. Meng, Z. Liu, Molecules **24**(4), 759 (2019)
[16] R. K. Tamrakar, D. P. Bisen, N. Brahme, Journal of Radiation Research and Applied Sciences **7**(4), 550 (2019).
[17] R. Priya, O. P. Pandey, S. J. Dhoble, Optics and Laser Technology **135**, 106663 (2021).
[18] S. J. Park, H. W. Jang, J. Y. Park, J. W. Chung, H. K. Yang, B. K. Moon, Ceramics International **45**(5), 5958 (2019).
[19] T. Gayathri, R. A. Kumar, S. Dhilipkumaran, C. K. Jayasankar, P. Saravanan, B. Devanand, Journal of Materials Science-Materials in Electronics **30**(7), 6860 (2019).
[20] A. Newport, G. R. Fern, T. Ireland, R. Withnall, J. Silver, A. Vecht, Journal of Materials Chemistry **11**(5), 1447 (2001).
[21] N. M. Maalej, A. Qurashi, I. Bennour, L. R. Haddada, M. N. Shaikh, M. Ilyas, N. E. Ben Amara, R. Maalej and M. A. Gondal, Methods and Applications in Fluorescence **9**(2), 025002 (2021).
[22] Kaminska, A. Wosztyl, P. Kowalik, B. Sikora, T. Wojciechowski, K. Sobczak, R. Minikayev, K. Zajdel, M. Chojnacki, W. Zaleszczyk, K. Lysiak, W. Paszkowicz, J. Szczytko, M. Baniewicz, W. Stryczniewicz, K. Fronc, Nanotechnology **32**(24), 33690193 (2021).
[23] F. Whba, F. Mohamed, N. Rosli, I. A. Rahman, M. I. Idris, Radiation Physics and Chemistry **179**, 109212 (2021).
[24] Upadhyay, S. Thomas, R. T. Varghese, R. K. Tamrakar, Polymer Testing **93**, 106911(2021).
[25] A. M. Kalinkin, V. Y. Vinogradov, E. V. Kalinkina, Inorganic Materials **57**(2), 178 (2021).
[26] V. Amendola, D. Amans, Y. Ishikawa, N. Koshizaki, S. Scire, G. Compagnini, S. Reichenberger, S. Barcikowski, Chemistry-a European Journal **26**(42), 9206 (2020).
[27] S. Zhang, J. Liu, P. F. Li, Z. F. Tian, C. H. Liang, Chemnanomat **3**(8), 512 (2017).
[28] Zhang, B. Gokce, S. Barcikowski, Chemical Reviews **117**(5), 3990 (2017).
[29] H. Zeng, X.-W. Du, S. C. Singh, S. A. Kulinich, S. Yang, J. He, W. Cai, Advanced Functional Materials **22**(7), 1333 (2012).

[30] D. Tan, S. Zhou, J. Qiu and N. Khusro, Journal of Photochemistry and Photobiology C: Photochemistry Reviews **17**, 50 (2013).
[32] Xiao, P. Liu, C. X. Wang, G. W. Yang, Progress in Materials Science **87**, 140 (2017).
[33] J. Liu, X. Tian, H. Chen, Y. Shao, G. Yang, D. Chen, Applied Surface Science **348**, 60 (2015).
[34] R. K. Tamrakar, K. Upadhyay, Journal of Electronic Materials **47**(1), 651 (2018).
[35] S. Wu, J. Yin, H. Qu, A. Li, L. Liu, Y. Shao, Journal of Materials Science: Materials in Electronics **30**(12), 11336 (2019).
[36] T. Yu, M. Y. Gao, H. M. Cheng, G. X. Liu, C. Song, X. T. Dong, J. X. Wang, W. S. Yu, Journal of Materials Science-Materials in Electronics **30**(17), 16376 (2019).
[37] Y. Liu, G. Liu, J. Wang, X. Dong, W. Yu, Inorganic Chemistry **53**(21), 11457 (2014).
[38] C. Cao, H. K. Yang, J. W. Chung, B. K. Moon, B. C. Choi, J. H. Jeong, K. H. Kim, Journal of Materials Chemistry **21**(28), 10342 (2011).
[39] Panigrahi, S. Saha, S. Sain, R. Chatterjee, A. Das, U. K. Ghorai, N. Sankar Das, K. K. Chattopadhyay, Dalton Transactions **47**(35), 12228 (2018).